Arab Journal of Physical Chemistry- http://aphyschem.org

Saudi Chemical Society

Article/ Awwad et al., Arab J. Phys. Chem., 1 (2) 2014, Page 65-70

Biosynthesis, characterization, and optical properties of magnesium hydroxide and oxide nanoflakes using *Citrus limon* leaf extract

Akl M. Awwad*, Ahmad L. Ahmad

Royal Scientific Society, El Hassan Science City, P.O. Box 1438 Amman 11941 Jordan, corresponding author's email: akl.awwad@yahoo.com, phone+962 6 5344701,fax number: +962 6 5344806.

Received 24 Sept. 2014,
Accepted 20 Oct. 2014

- **Novelty and Highlights:**

1 – Magnesium hydroxide and oxide nanoparticles are synthesized using *Citrus limon* leaf extract through green route.

2 –XRD and SEM patterns evinces the crystalline nature of the synthesized nanoparticles.

3 – Biomolecules of the *Citrus limon* leaf extract act as dispersing and capping agents.

- **Graphical Abstract:**

Green route for synthesized MgHNPs using *Citrus limon* leaf extract

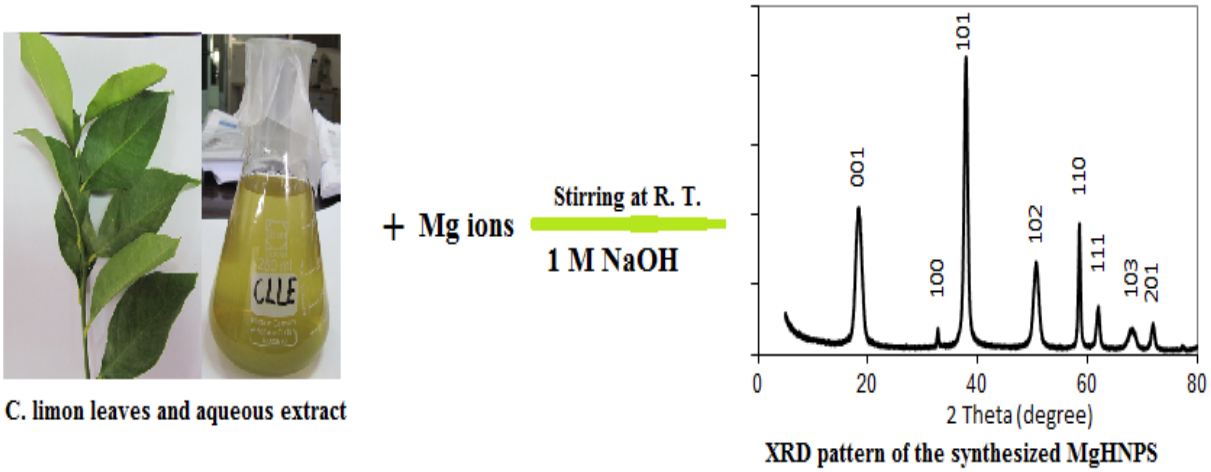

C. limon leaves and aqueous extract

XRD pattern of the synthesized MgHNPS

Arab Journal of Physical Chemistry- http://aphyschem.org

Saudi Chemical Society

Article/ *Awwad et al., Arab J. Phys. Chem., 1 (2) 2014, Page 65-70*

Biosynthesis, characterization, and optical properties of magnesium hydroxide and oxide nanoflakes using *Citrus limon* leaf extract

Akl M. Awwad*, Ahmad L. Ahmad

Royal Scientific Society, El Hassan Science City, P.O. Box 1438 Amman 11941 Jordan.
corresponding author's email: akl.awwad@yahoo.com, phone+962 6 5344701,fax number: +962 6 5344806.

Abstract: Magnesium hydroxide and oxide nanoparticles have been successfully synthesized from magnesium chloride and sodium hydroxide in presence of *Citrus limon* leaf extract in one-pot reaction at ambient temperature. The influence of synthesis parameters such as magnesium ion concentration, amount of Citrus limon leaf extract, reaction time, and temperature on the morphology characteristics and sizes of magnesium hydroxide nanoparticles was investigated. The amount ratio of plant leaf extract played an important role in determining the sizes of nanoparticles. The synthesized magnesium hydroxide and oxide nanoparticles were characterized by Fourier transforms infrared spectrophotometer (FT-IR), scanning electron microscopy (SEM), and X-ray diffraction (XRD). The UV-vis absorption spectrum shows an absorption band at 204 nm due to MgO nanoparticles and XRD characterize the final product as highly crystalline MgHNPs and MgONPs with nanoflakes size in the range of 12-80 nm.

Keywords: magnesium oxide, nanostructure, green chemistry.

Introduction

Magnesium hydroxide (Mg $(OH)_2$) and oxide (MgO) have been attracted much interest for its widely applications in flame retardant, filler in polymeric materials, environmental protection, antacid excipient in pharmaceuticals and foodborne pathogens. Therefore various methods for synthesis magnesium hydroxide and magnesium oxide nanoparticles have been reported in literature such as precipitation method [1-9], hydrothermal route [10,11], micro-emulsion method [12], wet co-precipitation process [13,14], ultrasonic synthesis [15,16], Laser ablation [17], spinning disk reactor [18], microwave-assisted synthesis [19] direct functionalization with non-ionic poly (ethylene glycols) [20] and sol-gel process [21]. These approaches have many disadvantages due to the difficulty of scale up of the process, separation and purification of nanoparticles from the oil, surfactant, and organic solvents. Developing green methods for synthesizing magnesium hydroxide and magnesium oxide nanoparticles are of importance and still a challenge for materials researchers. If the synthesis and production cost of magnesium hydroxide nanoparticles could be decreased greatly through using very cheap raw non-toxic materials, ambient temperature, large scale preparation, the practical application of magnesium hydroxide nanoparticles would be accessible. Thereby the new approach is not only green, economic, ecofriendly to environment and non-toxic by-products, but also easy to scale up.

Experimental

Materials and Methods

Magnesium chloride ($MgCl_2.6H_2O$) and sodium hydroxide (NaOH) were obtained from Aldrich and used as received without further purifications. Deionized distilled water was used in all experimental work.

Preparation of Citrus limon leaf extract.

Freshly plant leaves used in this work were collected from *Citrus limon* trees planted in Jordan and washed several times with distilled water to remove the dust particles and then dried to remove the residual moisture. The plant leaves extract used for synthesis magnesium hydroxide nanoparticles were prepared by placing 10 g of washed dried fine cut leaves in 250 mL glass beaker along with 400 mL of sterile distilled water. The mixture was then boiled for 10 minutes, the color of the aqueous solution changed from colorless to yellow color**.** Afterwards, the extract was cooled to room temperature and filtered by Whatman No. 1 filter paper before centrifuging at 1200 rpm for 5 minutes to remove the heavy biomaterials. The extracts were stored at room temperature in order to be used for the experimental work.

Synthesis of magnesium hydroxide nanoparticles.

In a typical reaction mixture, 1-20 ml of the aqueous yellow leaf extract of *Citrus limon* was added to 300 ml of 4 mM of aqueous magnesium chloride hexahydrate, $MgCl_2.6H_2O$ solution and stirred at room

temperature for 5 min to achieve pale yellow solution. Then 1M sodium hydroxide solution was added drop by drop to the mixture to adjust the pH 12-14, white suspended particles appeared, indicating the formation of magnesium hydroxide nanoparticles (MgHNPs). The suspended white particles solution was purified by dispersing in sterile distilled water and centrifugation three times. Afterwards, white particles were washed twice with pure ethanol and then dried at 80 ^{o}C to obtain white powder for FT-IR, XRD and SEM analysis. The above procedure was repeated by using different amounts of *Cirus limon* leaf extract and magnesium ions concentration at room temperature.

Characterization techniques.

Magnesium hydroxide nanoparticles synthesized by this green method were characterized by X-ray diffractometer, (XRD-6000, Shimadzu) equipped with Cu K α radiation source (λ =0.154056 nm) using Ni as filter at a setting of 30 kV/30mA. All XRD data were collected under the experimental conditions in the angular range $3^{o} \leq 2\theta \leq 50^{o}$. FT-IR spectra of leaf extract and synthesized MgHNPs were obtained in the range 4000-400 cm^{-1} with IR-Prestige 21 spectrophotometer (Shimadzu) using KBr pellet method. Scanning electron microscopy (SEM) images were taken using a field emission scanning electron microscopy (Hitachi S4700, 15 kV). UV–vis spectrum of magnesium oxide nanoparticles was recorded by a Schimadzu, 1601 spectrophotometer in the wavelength region 300 to 700 nm operated at a resolution of 1 nm.

Results and discussion

X-ray diffraction analysis, **Fig. 1 and 2** demonstrates the representative XRD pattern of the synthesized magnesium hydroxide nanoparticles, MgHNPs. The diffraction peaks with 2θ values of 18.08^{o}, 31.12^{o}, 37.84^{o}, 50.36^{o}, 58.52^{o}, 61.74^{o}, 67.08^{o} and 71.34^{o} correspond to reflections from (001), (100), (101), (102), (110), (111), (103) and (201) planes Bragg reflections, respectively. The unassigned peaks (*) at 2θ = 30.75^{o} and 45.25^{o} were also found along with the characteristic peaks. These Bragg peaks might have resulted due to crystalline and amorphous organic phase of *Citrus limon* leaf extract. Independent crystallization of the capping agents was ruled out due to the process of centrifugation and dispersion of particles in water after nanoparticle formation as part of purification process. Therefore XRD results also suggest that crystallization of the bioorganic phase occurs on the surface of the MgHNPs or vice versa. Generally, the broadening of peaks in the XRD pattern of solid is attributed to particle size effect. Broader peaks signify smaller particle size and reflect the effects due to experimental conditions on the nucleation and growth of the crystal nuclei. The mean crystallite size was calculated from the Debye-Scherrer equation [22]:

$$D = K\lambda/\beta cos\theta$$

Where, D is the crystallite size of MgHNPs, λ is the wavelength of x-ray source used in XRD, β is the full width at half maximum of the diffraction peak, K is the Scherrer constant with value from 0.9 to 1, and θ is the Bragg angle.

The mean crystallite size and the intensity ratio of reflections (001) to (101) for different samples (*I*001/*I*101were found to be dependent on the quantity of *Citrus limon* leaf extract mixed with magnesium ions. From the data in Table 1, It can be concluded that the mean crystallite size of MgHNPs depends on the amount of *Citrus limon* leaf extract.

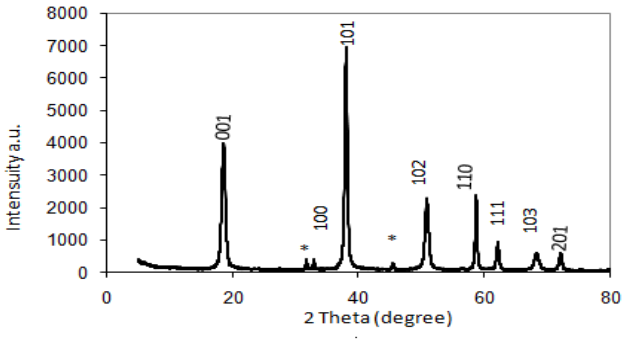

Fig. 1. XRD pattern of capped *Citrus limon* leaf extract – MgHNPs

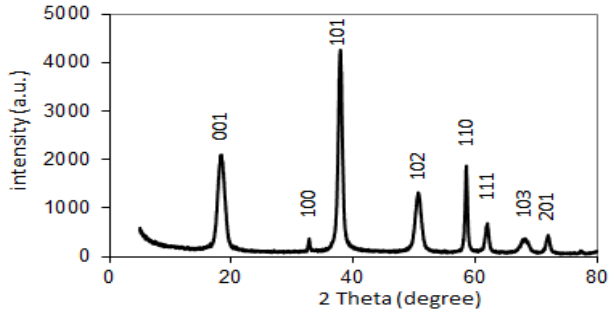

Fig. 2. XRD pattern of pure synthesized MgHNPs

Fourier transform infrared spectroscopy (FT-IR) was recorded to study the interaction between magnesium hydroxide and plant leaf extract. The *citrus limon* leaf extract displays a number of absorption peaks, reflecting its complex nature, Fig. 3. The band at 3371 cm^{-1} could be ascribed to the stretching absorption band of amino (-NH) and hydroxyl (–OH) groups.

Table 1. Mean crystallite size and *I*001/*I*101) for different samples.

Volume % of CLLE	Mean Crystallite size (nm)	*I*001/*I*101
1	80	0.52
3	60	0.74
6	40	0.98
9	22	1.24
12	12	1.98

The bands at 2920 cm^{-1} and 2850 cm^{-1} could be assigned to –CH stretching vibrations of $–CH_2$ and $-CH_3$ functional groups. The band at 1612 cm^{-1} is characteristic of amide I and amide II. The amide band I assigned to the stretch mode of the carbonyl group coupled to the amide linkage while the amide II band arises as a result of the N-H stretching modes of vibration in the amide linkage. The band at 1408 cm^{-1} is assigned to the methylene scissoring vibrations from the proteins. The strong band at 1026 cm^{-1} assigned to the C-O stretching vibrations of alcohols. Additional peaks at 775 $cm^{-1}$and 509 cm^{-1} can be assigned to bending modes of aromatic compounds. **Fig. 4** shows the FT-IR of the synthesized magnesium hydroxide nanoparticles. The sharp and intense peak at 3695 cm^{-1} can be attributed to the O-H stretching in the crystal structure of magnesium hydroxide nanoparticles. The broad band at 3406 cm^{-1} is attributed to surface adsorbed –OH groups of CLLE. This indicates that *Citrus limon* leaf extract serves to stabilize the crystal growth of the particles and thus control the size of the particles and prevent agglomeration of the particles..

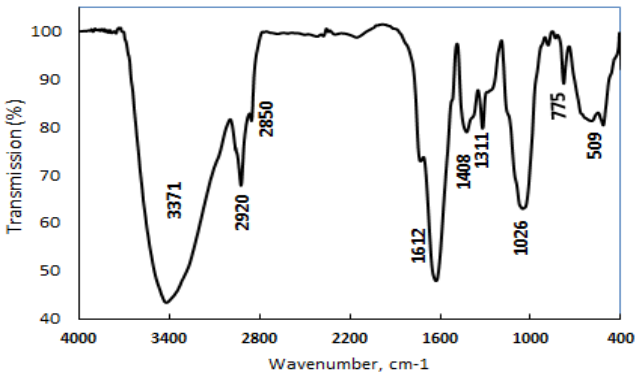

Fig. 3. FT-IR spectra of *Citrus limon* leaf extract

The strong band at 444 cm^{-1} is assigned to Mg-O stretching vibration in MgHNPs. FT-IR results indicate that *Citrus limon* leaf extract act as dispersing, capping and stabilizing agent for the synthesized MgHNPs.

Fig. 5 shows the SEM image of the synthesized magnesium hydroxide nanoparticles. It can be seen from the image that magnesium hydroxide particles display flakes shape. The mean width of magnesium hydroxide was about 80 nm. The mean crystallite size is found to be larger than that obtained by XRD analysis and this is probably due to aggregation of the particles.

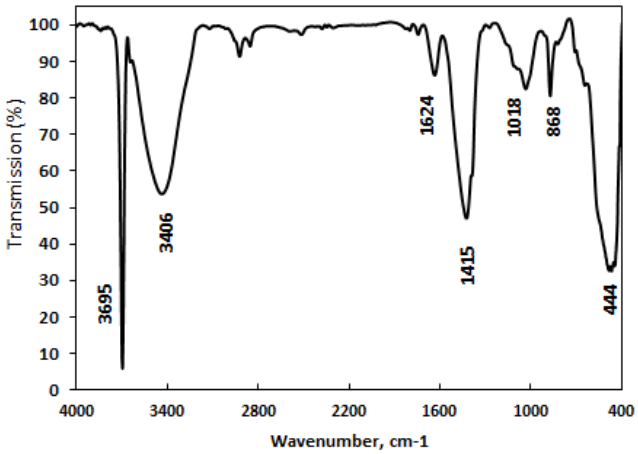

Fig. 4. FT-IR spectra of MgHNPS-capped by *Citrus limon* leaf extract.

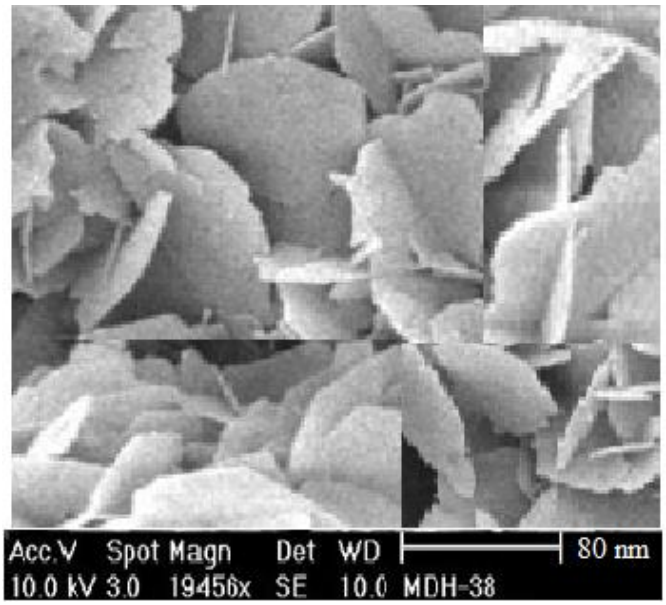

Fig. 5. SEM image of the synthesized magnesium hydroxide nanoparticles.

Synthesized magnesium hydroxide nanoflakes (MgONPs) was annealed at 750°C for 3h in a muffle furnace. MgO particles produced were characterized by X-ray diffraction (XRD) and scanning electron microscopy (SEM). **Fig. 6** demonstrates the representative XRD pattern of the magnesium oxide nanoparticles, MgONPs. The diffraction peaks with 2θ values of 36.51°, 42.22°, 61.52°, 73.48° and 78.18°

correspond to reflections from (111), (200), (220), (331), and (222) planes Bragg reflections, respectively. No extra diffraction peaks of other phases are detected, indicating the phase purity of MgO nanoparticles. The average crystallite size of the synthesized magnesium oxide nanopwder was calculated to be 20 nm by using Debye-Scherrer equation.

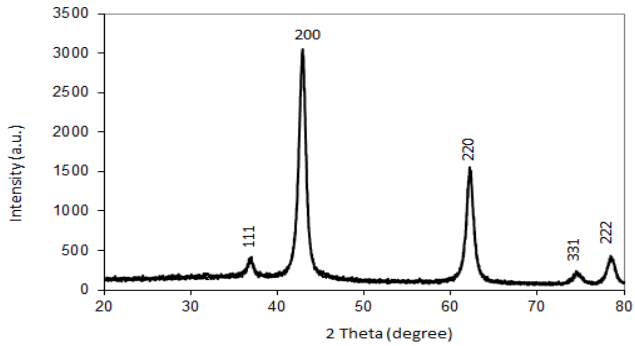

Fig. 6. XRD pattern of MgONPs

UV-vis of the synthesized MgO nanoparticles is shown in **Fig. 7.** An absorption peak was observed in each spectrum at 204 nm which is characteristic band for pure magnesium oxide. No other peaks were observed in the spectrum, indicating the high purity of the synthesized magnesium oxide nanoparticles.

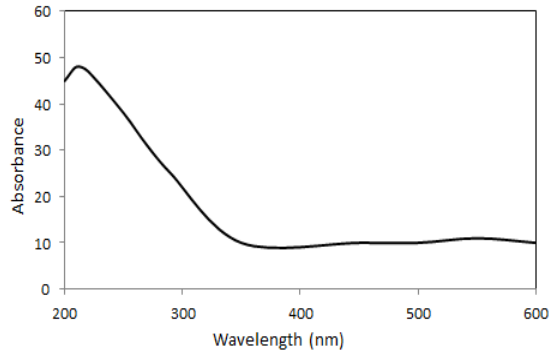

Fig.7. UV-Vis of synthesized magnesium oxide nanoparticles

The energy band gap can be estimated by assuming direct transmission between conduction and valance bands. The relation between the absorption coefficient (α) and photon energy (hν) for direct transmission by the following relation [23]:

$\alpha^2 = (C/h\nu)\ (h\nu - E_g)^{1/2}$

or

$(h\nu\alpha)^2 = C\ (h\nu - E_g)$

Where E_g is the direct optical band energy, *hν* is the incident photon energy, α is absorption coefficient, and C is a constant. The energy band gap (E_g) can be obtained by plotting $(\alpha h\nu)^2$ versus photon energy (hν) and extrapolating the linear portion of the curve to the photon energy axis. From the plot, **Fig. 8** the direct energy band gap is calculated was found to be 4.2 ev, from the extrapolation to linear line of the curve.

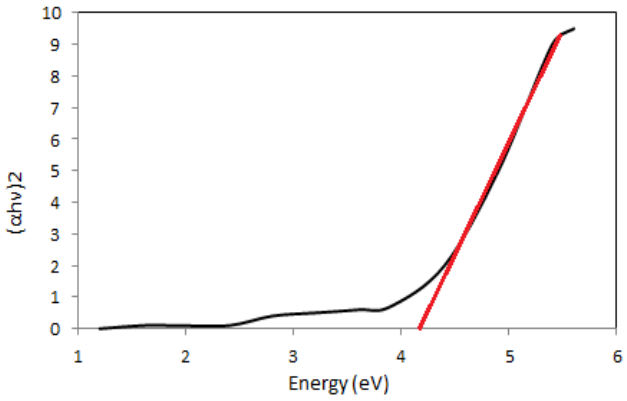

Fig. 8. Plot of $(\alpha h\nu)^2$ versus (hν) of synthesized magnesium oxide nanoparticles

FT-IR of MgONPs is shown in **Fig.9.** This clearly shows a broad absorption band at 3393 cm^{-1}, which is the characteristic stretching vibration of the hydroxyl group (-OH). Strong peak localized at 1415 cm^{-1} is due to aromatic ring in the *Citrus limon* leaf extract. The absorption bands at 860 cm^{-1} is attributed to the absorption peak of MgO. The strong absorption at 490 cm^{-1} is the stretching vibration of Mg-O.

The SEM micrograph in **Fig. 10** demonstrates that, during magnesium hydroxide nanoplates calcination at 750 ^oC and oxide formation, the plate-like shape of the particles persists, even though it is a nonequilibrium shape for MgO. At high temperature, the platelets break into isometric particles.

Conclusions

A new and green route has been developed for synthesis magnesium hydroxide and oxide nanoparticles in one-pot reaction process at ambient temperature. Our synthesis approach employed an environmental friendly biomaterial, *Citrus limon* leaf extract, as an alternative to organic solvents and surfactants. Citrus limon acts as dispersing and stabilizing agent, which prevents the agglomeration of magnesium hydroxide nanoparticles (MgHNPs) formed during synthesis. Calcination of syhthesized MgHNPS at 750 ^oC converted to MgO

plate-like. XRD and SEM data showed that the size and shape of the magnesium hydroxide and oxide nanoparticles could be controlled by the amount of *Citrus limon* leaf extract and the concentration of Mg(II) ions. The method in the present study offers several important advantageous features. 1. The synthesis method is eco-friendly and economical, because it involves inexpensive and non-toxic materials, 2. Size-controlled magnesium hydroxide and magnesium oxide nanoparticles are produced easily by different amounts of *Citrus limon* leaf extract, 3. Scale up the process.

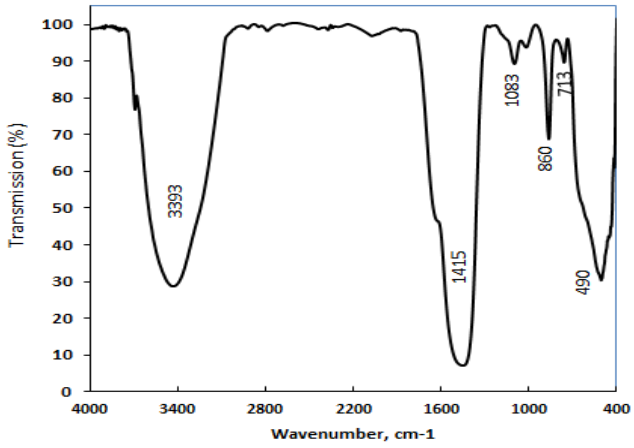

Fig. 9. FT-IR of magnesium oxide nanoparticles

Fig. 10. SEM of magnesium hydroxide calcined at 750°C.

Acknowledgment
The authors would like to thank Royal Scientific Society, El Hassan Science City, Jordan for providing all facilities to carry out this work.

Notes and References

1. P. Wang, C. Li, H. Gong, H. Wang, J. Liu, Ceramics Inter. 2011, **37**, 3365.
2. D. An, L. Wang, Y. Zheng, S. Guan, X. Gao, Y. Tian, H.Z. Wang, Y. Liu, Colloids and Surfaces A: Physicochemical and Eng. Aspects 2009, **348**, 9.
3. C. Henrist, J.P. Mathieu, C. Vogels, A. Rulmont, R. Cloots, Journal of Crystal Growth 2002, **249**, 321.
4. L.V. Jianping, L. Qiu, B. Qu, J. of Crystal growth 2004, **267**, 676.
5. D. An, X. Ding, Z. Wang, Y. Liu, Colloids and Surfaces A: Physicochemical and Engineering Aspects 2010, **356**, 28.
6. W. Jiang, X. Hua, Q. Han, X. Yang, L. Lu, X. Wang, Powder Technology 2009, **191**, 227.
7. A. Pilarska, M. Wysokowski, E. Markiewicz, T. Jesionowski, Powder Technology 2013, **235**, 148.
8. X. Song, S. Sun, D. Zhang, J. Wang, J. Yu, Frontiers Chemical Science and Engineering 2011, **5**, 416.
9. F. Meshkani, M. Rezaei, Powder Technology 2009, **196**, 85.
10. H. Yan, X-h. Zhang, J-m. Wu, L-q. Wei, B-s. Xu, Powder Technology 2009, **188**, 128.
11. X.T. Sun, L. Xiang, Materials Chemistry and Physics 2008, **109**, 381.
12. J. Wu, H. Yan, X. Zhang, L. Wei, X. Liu, B.; Xu, Journal of Colloid and Interface Science 2008, **324,** 167.
13. D. Chen, L. Zhu, P. Liu, H. Zhang, K. Xu, M. Chen, Journal of Porous Materials 2009, **16**, 13.
14. D. Chen, L. Zhu, H. Zhang, X. Xu, M. Chen, Materials Chemistry and Physics 2008, **109**, 224.
15. G. Song, S. Ma, G. Tang, X. Wang, Colloids and Surfaces A: Physicochemical and Engineering Aspects 2010, **364**, 99.
16. M.A. Alavi, A. Morsali, Ultrasonics Sonochemistry 2010, **17**, 441.
17. T.X. Phuoc, B.H. Howard, D.V. Martello, Y. Soong, M.K. Chyu, Optics and Lasers in Engineering 2008, **46**, 829.
18. C.Y. Tai, C-T. Tai, M-H Chang, H-S. Liu, Industrial & Engineering Chemistry Research 2007, **46**, 5536.
19. S. Makhluf, R. Dror, Y. Nitzan, Y. Abramovich, R. Jelinek, A. Gedanken, Advanced Functional Materials 2005, **15**, 1708.
20. A. Pilarska, I. Linda, M. Wysokowski, D. Paukszta, T. Jesionowski, Physicochem. Probl. Miner. Process 2012, **48**, 631.
21. R. Wahab, S.G. Ansari, M.A. Dar, Y.S. Kim, H.S. Shin, Materials Science Forum 2007, **558-559**, 983.
22. H.P. Klug, L.E. Alexander, 2001; X-ray diffraction procedures, Wiley/Interscience, New York.
23. B.K. Sonawane, V. Shelke, M.P. Bhole, D.S. Patil, Journal of Physics and Chemistry of Solids 2011, **72**, 1442.